HBV/HCV Infection Model Using Cultured Cells. The plasmid pHBV 1.2 coding the 1.2-fold length of the HBV genome was transfected into Huh7.5 cells using Fugene6 transfection reagent (Roche Applied Science, Indianapolis, IN). HBeAg production in culture medium was measured using Immunis HBeAg/Ab EIA (Institute of Immunology Co., Ltd., Tokyo, Japan).[13] The amount of HBV-DNA was measured via RTD-PCR (Supplementary Fig. 1A,B). JFH1-RNA was transfected into Huh7.5 cells using TransMessenger transfection reagent (QIAGEN) and the expression of the core protein was examined via immunofluorescence staining using anti-HCV core antibody (Affinity BioReagent, CO).[14,15] HCV-RNA amount was also measured via RTD-PCR (Supplementary Fig. 1A,B). JFH1/GND was used as a negative control. miRNA expression was quantitated by RTD-PCR 48 hours after transfection.

Results

Expression of miRNA in Liver Tissue. A panel of miRNA was successfully amplified from liver tissues via RTD-PCR. The representative amplification profile of miRNA as determined with RTD-PCR is shown in Fig. 1. To assess the reliability and reproducibility of this assay system, we first measured RNU6B in duplicate from all samples in different plates. The mean difference in Ct values of RNU6B expression within the same samples was 0.08 ± 0.05 (mean ± standard deviation), indicating the high reproducibility of this assay. All Ct values from each reaction were collected, and Ct variation obtained by each probe from all patients was calculated. Although RNU6B was frequently used as the internal control, the standard Ct variation was relatively high (Ct, 27 ± 1.94), suggesting that the variances in its value depend on the state of liver disease (N, CH and HCC). Therefore, we selected has-miR-328 as the internal control with the smallest standard deviation (Ct, 30 ± 0.60). The relative expression ratio of individual miRNA to has-miR-328 was calculated and applied to the following analysis using a BRB-array tool.

Hierarchical cluster analysis revealed that the expression profiles of the 188 miRNAs from each patient were roughly classified into normal liver, HBV-infected liver (CH-B+HCC-B; HBV group), and HCV-infected liver (CH-C+HCC-C; HCV group) (Fig. 2A). HCV viremia in two patients with CH-C was persistently cleared by interferon therapy before HCC development. The background liver of one of these patients was clustered in the normal group and those of others in the HCV group. Although these two patients were not clearly differentiated from others, some miRNAs such as miR-194, miR-211, and miR-340 that were down-regulated in the HCV group were significantly up-regulated in two patients (Fig. 3, cluster 2).

The present CH and HCC expression data were obtained from the same patient; however, each sample clustered irrespective of pairs in all but two patients. miRNA expression profiling was therefore more dependent on the disease condition than on the paired condition, as also confirmed by the Dunnett test.[12] We then attempted to classify the expression profiles into HBV and HCV groups using supervised learning methods (Table 2-1). HBV and HCV groups were significantly differentiated at an 87% accuracy ($P < 0.001$). The normal liver and CH (CH-B + CH-C) and CH and HCC (HCC-B + HCC-C) were also significantly differentiated at a 90% rate of accuracy. These results suggest that different stages of liver disease (normal, CH, and HCC) can be differentiated from each other based on the miRNA expression profile, as well as HBV and HCV infection.

To examine the relationship among five categories of groups, namely, N, CH-B, CH-C, HCC-B and HCC-C, we attempted to differentiate the five groups using a supervised learning algorithm (binary tree classification) used for classifying three or more groups. SVM was used as a prediction method. Expression profiles were first classified into groups N (normal) and non-N (non-normal) (CH-C, CH-B, HCC-C, and HCC-B) (node 1) ($P < 0.01$). The non-N group was then classified into HBV and HCV (node 2) ($P < 0.01$). The HBV group was further classified into CH-B and HCC-B (node 3) ($P < 0.01$), and the HCV group was further classified into CH-C and HCC-C (node 4) ($P < 0.01$) (Fig. 2B, Table 2-2). Thus, the findings support the notion that differences in miRNA expression between HBV and HCV are as distinct as those between CH and HCC.

Out of 20 miRNAs that differentiated node 1 classification (Table 2-2), 12 also differentiated node 3 or node 4 classification. The remaining eight miRNAs specifically differentiated node 1 classification. They were down-regulated in the HBV and HCV groups compared with the normal group (Fig. 3, cluster 1). Nineteen miRNAs differentiated node 2 classification (Table 2-2) and the hierarchical clustering using these miRNAs clearly differentiated the HBV and HCV groups (Fig. 3, cluster 2). There were 15 and 14 miRNAs that differentiated node 3 and 4 classifications, respectively (Table 2-2). Hierarchical clustering using these miRNAs revealed that these miRNAs differentiated CH-B and HCC-B as well as CH-C and HCC-C, respectively; 17 miRNAs were down-regulated in HCC, and six were up-regulated in HCC (Fig. 3, cluster 3).

Table 3-2. Differentially Expessed miRNA Between HCC-B, CH-B, and HCC-C, CH-C, and Their Representative Target Genes (Cluster 2)

miRNA	Parametric P Value	Ratio*	No. of Significant Genes/Predicted Target Genes†	Hotelling Test P Value‡	Differentially Expressed Target Genes§	Pathway of Regulated Genes¶
hsa-miR-190	1.2E-05	2.06	21/68	4.47E-02	Chk1, C2orf25, VRK2, USP16, STAF65(gamma)	Regulation of cell cycle
					AP1S2, RNASE4	Mitotic cell cycle
					PPP2R1B, ARHGAP15, UBPY	Negative regulation of apoptosis
hsa-miR-134	2.3E-04	5.74	11/58	3.40E-06	VKDGC, SH2B, MALS-1, DDB2	Multicellular organismal process
					BCRP1	Regulation of viral reproduction
					DDB2	Lipid biosynthetic process
hsa-miR-151	2.8E-04	1.82	12/62	6.41E-01	RGS2, UFO, AK2, USP7	G-protein signaling
					eIF4G2, USP7	Regulation of translation
					SLC22A7	Organic anion transport
hsa-miR-193	5.0E-04	1.67	23/95	9.30E-01	G-protein alpha-11, p130CAS, VAV-1, PDCD11	Cell motility
					Colipase, ACSA	Energy coupled proton transport
					DCOR	Intracellular signaling cascade
hsa-miR-133b	1.7E-03	2.42	20/97	3.69E-02	DDB2, Bcl-3, Cystatin B	Proteasomal protein catabolic process
					Rab-3, RAG1AP1, KCNH2, DCOR	Regulation of biological quality
					AL1B1	Carbohydrate metabolic process
hsa-miR-324-5p	2.9E-03	1.51	27/121	1.90E-06	SKAP55, VAV-1, DDB2, E2A, NIP1	Cellular developmental process
					MEMO (CGI-27), Rab-3	Cellular structure morphogenesis
					COPG1, GPX3, OAZ2	Glutathione metabolic process
hsa-miR-182*	3.1E-03	2.23	28/123	< 1e-07	Alpha-endosulfine, HCCR-2, Thioredoxin-like 2, TPT1, USP7	Translation initiation in response to stress
					DDB2, TPT1	Cellular developmental process
					JIP-1	JNK cascade
hsa-miR-105	4.6E-03	4.38	18/68	4.74E-05	Beta-2-microglobulin, HLA-B27	Antigen processing and presentation
					PIMT, IL-17RC	Immune response
					MHC class I, CDK9, ERG1, Desmocollin 3	
hsa-miR-211	5.3E-03	25.61	10/56	2.00E-04	PSMD5, SLC26A6	Proteasomal protein catabolic process
hsa-miR-20	5.7E-03	1.52	27/113	5.28E-03	Noelin, SC4MOL, Thioredoxin-like 2, CCL5, NALP3	Regulation of apoptosis
					Hic-5/ARA55, USP16, MAP4, Ferroportin 1	Positive regulation of cellular process
					TOP3A, PLRP1	Oxygen transport
hsa-miR-191	6.7E-03	1.39	25/79	7.55E-04	CDK9, GPS2, CLTA, LXR-alpha	Nucleic acid metabolic process
					ACSA	Acetyl-CoA biosynthetic process
					UGCGL1, SGPP1	Metal ion transport
hsa-miR-340	8.5E-03	1.48	17/81	3.73E-03	FKBP12, DCOR,	Calcium ion transport
					Gelsolin, VAV-1, ARF6	Actin cytoskeleton organization and biogenesis
					HXK3	Glucose catabolic process
hsa-miR-194	8.7E-03	1.67	13/74	5.90E-01	Cyclin B1, Serglycin	M phase of mitotic cell cycle
					PTE2	Acyl-CoA metabolic process
					SLC7A6	Carbohydrate utilization
hsa-miR-23a	1.9E-04	0.46	14/97	< 1e-07	*RGL2*, MANR, MEK1 (MAP2K1), Caspase-3, AZGP1	Protein kinase cascade
					FRK, Pyk2(FAK2), CSE1L	Cellular developmental process
					AZGP1	Defense response
hsa-miR-142-5p	4.9E-04	0.40	25/89	9.10E-06	Sirtuin4, PAI2, PSAT, RIL, CDC34, SPRY1	Metabotropic glutamate receptor
					E4BP4, DNAJC12, WWP1, PAIP1, PASK, rBAT	Regulation of gene expression
					VCAM1, CaMK I, WWP1, FHL3	Cell-matrix adhesion
hsa-miR-34c	5.1E-04	0.20	31/129	7.30E-06	Diacylglycerol kinase, zeta, PLC-delta 1, ATP2C1, PAI2	Manganese ion transport
					MLK3(MAP3K11), MEK1(MAP2K1), CDC25C, MRF-1, XPC	Protein kinase cascade
					GNT-IV	Inflammatory cell apoptosis

Table 3-2. Continued

miRNA	Parametric P Value	Ratio*	No. of Significant Genes/Predicted Target Genes†	Hotelling Test P Value‡	Differentially Expressed Target Genes§	Pathway of Regulated Genes¶
hsa-miR-124b	8.6E-04	0.32	25/120	7.10E-05	E2F5, Rad51, Jagged1	Muscle development
					MLK3(MAP3K11), RGS1	Intracellular signaling cascade
					COL16A1	MAPKKK cascade
hsa-let-7a	1.0E-03	0.45	28/136	9.35E-04	RAD51C, CoAA, hASH1, Cockayne syndrome B, Caspase-1, PP5	Response to DNA damage stimulus
					PLC-delta 1, MANR, ACADVL	Fibroblast proliferation
					HGF, NGF	Cellular developmental process
hsa-miR-27a	3.9E-03	0.59	18/108	1.19E-02	COL16A1, RIL, RhoGDI gamma, ANP32B (april)	Cytoskeleton organization and biogenesis
					VE-cadherin, NTH1, GATA-2, E4BP4	Response to external stimulus
					RAD51C	DNA recombination

*Ratio of HCC-B, CH-B, to HCC-C,CH-C.
†The number of significant genes ($p < 0.05$) out of predicted target genes in which expression was evaluated in microarray.
‡Statistical assesment of presence of differentially expressed genes out of predicted target genes of miRNAs.
§Representative differentially expressed genes out of predicted target genes of miRNAs.
¶Representative pathway of differentially expressed genes out of predicted target genes of miRNAs.

These results indicate that there were two types of miRNAs—one associated with HBV and HCV infection (cluster 2), the other associated with the stages of liver disease (clusters 1 and 2) that were irrelevant to the differences in HBV and HCV infection.

Differential miRNAs and Their Candidate Target Genes and Signaling Pathways. Differentially expressed miRNAs are shown in Table 3. In addition to the expression ratios of miRNAs in each group, the number of genes analyzed on the microarray predicted to be the target genes of miRNAs and that which actually showed significant ($P < 0.05$) differences in expression are also shown. Based on the frequencies and levels of expression of differential genes, the significance of regulation of these gene groups by miRNAs was evaluated using Hotelling T2 test (BRB ArrayTools) (Table 3). The representative candidate target genes and their signaling pathways by each miRNA were shown one by one (Table 3). The signaling pathways regulated by all differential miRNAs in each category of groups are shown in Table 4.

Eight miRNAs were down-regulated in the HBV and HCV groups compared with the normal group (Table 3-1; Fig. 3, cluster 1). These miRNAs were associated with an increased expression of genes related to cell adhesion, cell cycle, protein folding, and apoptosis (Tables 3-1, 4-1), and possibly with the common feature of CH irrespective of the differences in HBV and HCV infection.

Nineteen miRNAs clearly differentiated the HBV and HCV groups (Fig. 3, cluster 2, Table 3-2). Thirteen miRNAs exhibited a decreased expression in the HCV group, and six showed a decreased expression in the HBV group. miRNAs exhibiting a decreased expression in the HCV group regulate genes related to immune response, antigen presentation, cell cycle, proteasome, and lipid metabolism. On the other hand, those exhibiting a decreased expression in the HBV group regulate genes related to cell death, DNA damage and recombination, and transcription signals. These findings reflected the differences in the gene expression profile between CH-B and CH-C described (Tables 3-2, 4-2).[10] Interestingly, although these miRNAs were HBV and HCV infection–specific, some of them were reported to be tumor-associated miRNAs, suggesting the possible involvement of infection-associated miRNAs in HCC development.

Twenty-three miRNAs clearly differentiated CH and HCC that were irrelevant to the differences in HBV and HCV infection. Seventeen miRNAs were down-regulated in HCC that up-regulated cancer-associated pathways such as cell cycle, adhesion, proteolysis, transcription, translation, and the Wnt signaling pathway (Tables 3-3, 4-3). Six miRNAs were up-regulated in HCC that down-regulated all inflammation-mediated signaling pathways, potentially reflecting impaired antitumor immune response.

Relationship Between Expressions of Infection-Associated miRNA in Liver and Cultured Cells Infected with HBV and HCV. To clarify whether the expression of infection-associated miRNA is regulated by HBV and HCV infection, we investigated the relationship between changes in miRNA in liver tissues and those in miRNA in Huh7.5 cells in which infectious HBV or HCV clones replicated. To evaluate the replication of each clones in Huh7.5 cells, we measured time-course changes in the amounts of HBV-DNA and HCV-RNA in Huh7.5 cells transfected with pHBV1.2 and JFH1-RNA, respectively, by RTD-PCR (Supplementary Fig. 1A). The expression of HBV proteins was examined by measuring the amount

Table 3-3. Differentially Expessed miRNA Between CH and HCC and Their Representative Target Genes (Cluster 3)

miRNA	Parametric p-value	Ratio*	No. of Significant Genes/Predicted Target Genes†	Hotelling Test *P* Value‡	Differentially Expressed Target Genes§	Pathway of Regulated Genes¶
hsa-miR-139	4.50E-06	0.42	19/106	2.70E-03	Cyclin B1, DHX15, MCM5, Histone H2A	Mitotic cell cycle
					RBCK1, SYHH	Protein catabolic process
					ILK, IGFBP7, SAFB, CTR9	Response to external stimulus
hsa-miR-30a-3p	2.50E-05	0.49	26/144	1.73E-02	GGH, Pirin, ZNF207, Annexin VII	Regulation of oxidoreductase activity
					ILK, LTA4H, ABC50, GNPAT	Cell-matrix adhesion
					DLC1	Morphogenesis
hsa-miR-130a	7.00E-05	0.50	22/108	1.07E-02	SPHM, PPP2R5D, RHEB2, SPHM	Mitotic cell cycle
					MLK3(MAP3K11), Otubain1, TIMP4	Protein modification process
					NRBP	Cell differentiation
hsa-miR-223	3.40E-04	0.39	14/90	6.52E-03	Ephrin-A1, Midkine, FDPS	Cell morphogenesis
					K(+) channel, subfamily J	Notch signaling pathway
hsa-miR-187	3.55E-04	0.12	16/66	6.76E-04	HFE2, Otubain1	Negative regulation of programmed cell death
					PRSS11, SUPT5H, RAG1AP1	Developmental process
					PLOD3	Mitochondrial ornithine transport
hsa-miR-200a	6.86E-04	0.18	20/141	2.15E-02	*CDC25B, KAP3, CDK2AP2,* CHKA	Cell communication
					POLD	DNA replication
					CPSF4	RNA splicing
hsa-miR-17-3p	8.42E-04	0.58	28/108	8.98E-04	MLK3(MAP3K11), Tip60, ACBD6, DOC-1R, DAX1, RBCK1	Protein kinase cascade
					WNT5A, 14-3-3 gamma, DHX15	BMP signaling pathway
					HFE2, MCM5	DNA recombination
hsa-miR-99a	1.17E-03	0.53	33/163	9.52E-03	Calpain small subunit, Thoredoxin-like 2, Survivin	Cytokinesis
					IBP2, DNA-PK, KAP3,	Intracellular signaling cascade
					NFE2L1, PARP-1, HDAC11	Regulatory T cell differentiation
hsa-miR-200b	1.57E-03	0.18	24/147	2.72E-02	HSP47, HMG2, NRBP	Regulation of cell cycle
					SNX17	Cell motility
					Ephrin-A1	Receptor protein signaling pathway
hsa-miR-125b	1.82E-03	0.55	26/114	1.03E-01	COL4A2, TIP30, HSP47, MSP58	Cell adhesion
					MLK3(MAP3K11), ERK2 (MAPK1), ERK1 (MAPK3), PLOD3	Nuclear translocation of MAPK
					Otubain1, SCN4A(SkM1)	Ubiquitin-dependent protein catabolic process
hsa-miR-30e	2.10E-03	0.65	24/151	4.30E-02	Cyclin B1, XTP3B, GAK, Annexin VII, MIC2, NRBP	Mitotic cell cycle
					MSS4	Protein localization
					S100A10	Calcium ion transport
hsa-miR-199a*	4.26E-03	0.35	11/71	7.16E-02	BUB3, Cyclin B1, LMNBR	Mitotic cell cycle
					PRAME	Cardiac muscle cell differentiation
hsa-miR-122a	6.31E-03	0.51	11/80	1.01E-03	JAB1, APEX, Clathrin heavy chain	Base-excision repair
					PARN	Translational initiation
					DDAH2	Regulation of cellular respiration
hsa-miR-199a	8.77E-03	0.35	18/94	3.56E-02	IL-13, MLK3(MAP3K11), CLK2, ACP33	Protein amino acid phosphorylation
					PAFAH beta, SPA1, CLCN4	Small GTPase mediated signal transduction
hsa-miR-326	9.00E-03	0.57	29/147	2.25E-01	Midkine, ENT1, IP3KA, PSMC5, ANCO-1	Regulation of programmed cell death
					Thy-1, MCM6, Tip60, VILIP3	Cell-matrix adhesion
					COMP, Cathepsin A	Blood vessel development
hsa-miR-92	9.60E-03	0.81	28/140	2.47E-02	*TUBGCP2,* Fibrillin 1, PIPKI gamma, KAP3	Rho protein signal transduction
					SNX15, BCAT2	LDL receptor and BCAA metabolism
					IGFBP7, FZD6, COPS6	Adenosine receptor signaling pathway
hsa-miR-221	3.40E-06	3.34	16/67	3.59E-01	Lck, Kallistatin, Neuromodulin, LFA-3, PA24A, AZGP1, MSH2	Immune response-activating signal transduction
					KYNU, PMCA3	DNA repair

Table 3-3. *Continued*

miRNA	Parametric p-value	Ratio*	No. of Significant Genes/Predicted Target Genes†	Hotelling Test *P* Value‡	Differentially Expressed Target Genes§	Pathway of Regulated Genes¶
hsa-miR-222	6.50E-06	2.23	18/85	1.59E-02	Thrombospondin 1, Lck, MSH2, ATF-2, CITED2, Kallistatin	Cell motility
					PGAR	Triacylglycerol metabolic process
					KYNU	DNA replication
hsa-miR-301	5.22E-05	1.96	14/71	1.16E-01	Beta-2-microglobulin, PPCKM, PRC, Fra-1, PPCKM, ACAT2	Antigen processing and presentation
					BMPR1B, ARMER, EHM2, RBBP8	Meiotic recombination
					Neuromodulin, LDLR	Cell motility
hsa-miR-21	7.67E-03	1.57	19/81	1.86E-04	Btk, Fra-1, MSH2, Collectrin, Adipophilin	Regulation of T cell proliferation
					RNASE4, AGXT2L1	Peptidyl-tyrosine phosphorylation
					SARDH	Natural killer cell activation during immune response
hsa-miR-183	2.46E-02	3.51	13/86	3.36E-01	Hdj-2, PEMT, Lck, MKP-5, Chondromodulin-I, ABCA8	Cell differentiation
					IL-16, MTRR, SerRS	Methionine biosynthetic process
hsa-miR-98	5.22E-02	1.32	24/130	2.95E-04	ACAA2, LTB4DH, ACADVL, DECR, S14 protein,	Fatty acid metabolic process
					Rapsyn, Kallistatin, ENPEP, Beta crystallin B1	Multicellular organismal process
					CYP4F8	Prostaglandin metabolic process

*Ratio of HCC to CH.

†The number of significant genes ($P<0.05$) out of predicted target genes in which expression was evaluated in microarray.

‡Statistical assesment of presence of differentially expressed genes out of predicted target genes of miRNAs.

§Representative differentially expressed genes out of predicted target genes of miRNAs.

¶Representative pathway of differentially expressed genes out of predicted target genes of miRNAs.

of HBeAg released in culture medium (Supplementary Fig. 1B). HCV protein expression was examined by evaluating the core protein expression after 48 hours by fluorescence immunostaining (Supplementary Fig. 1C). RNA was extracted from the Huh7.5 cells 48 hours after gene transfection, and miRNA expression pattern in the cells was compared with those in liver tissues. We found a strong correlation between differences in miRNA expression between liver tissues of the HBV and HCV groups, and those in miRNA expression between Huh7.5 cells transfected with HBV and HCV clones ($r = 0.73$, $P = 0.0006$) (Fig. 5). These results revealed that differences in the expression of infection-associated miRNA in the liver between the HBV and HCV groups are explained by changes in miRNA expression caused by HBV and HCV infections.

Verification of Regulation of Candidate Target Genes by miRNA. Anti-miRNAs (Ambion) specific to 13 miRNAs (has-miR-17*, has-miR-20a, has-miR-23a, has-miR-26a, has-miR-27a, has-miR-29c, has-miR-30a, has-miR-92, has-miR-126, has-miR-139, has-miR-187, has-miR-200a, and has-miR-223) showing significant differences in expression were transfected into Huh7 cells to examine loss of function of the miRNAs. Five miRNAs (has-miR-23a, has-miR-26a, has-miR-27a, has-miR-92, and has-miR-200a) showed a decreased expression by more than 50%. Precursor miRNAs of these miRNAs were also transfected into the cells to examine the gain of function of the miRNAs (Supplementary Fig. 2). It was confirmed that the expressions of target genes of the five miRNAs (LIG4 [by has-miR-26a]; RGL2 [by has-miR-23a]; Rad51C [by has-miR-27a]; KAP3, CDC25B, KAP3, CDK2AP2, POLD, and CPSF4 [by has-miR-200a]; and TUBGCP2, SNX15 and BCAT2 [by has-miR-92]) were increased by the suppression of the miRNAs induced by anti-miRNAs and were decreased by the overexpression of precursor miRNAs (Supplementary Fig. 3).

Discussion

miRNA plays an important role in various diseases such as infection and cancer.[1-3] In this study, we examined miRNA expression profiles in normal liver and HCC, including nontumor lesions infected with HBV or HCV. Although the expression profiles of miRNAs in HCC have been reported,[16-18] most of the studies were performed using a microarray system. Because we thought that miRNAs could not produce enough detection signals owing to their short length, we applied a highly sensitive and quantitative RTD-PCR method for miRNAs. Moreover, global gene expression in the same tissues was ana-

Table 4-1. Pathway Analysis of Targeted Genes by miRNAs that Were Commonly Repressed in CH-B, CH-C, HCC-B, and HCC-C Compared with Normal Liver (Cluster 1)

No.	Pathway Name	*P* Value
Down-regulated miRNA in CH-B,HCC-B,CH-C and HCC-C (possibly up-regulating target genes)		
1	Cell adhesion_Platelet-endothelium-leukocyte interactions	1.11E-02
2	Cell cycle_S phase	2.18E-02
3	Protein folding_Protein folding nucleus	2.43E-02
4	Cell cycle_G1-S	3.07E-02
5	Development_Cartilage development	3.89E-02
6	Protein folding_Folding in normal condition	3.89E-02
7	Proteolysis_Connective tissue degradation	3.99E-02
8	Proteolysis_Proteolysis in cell cycle and apoptosis	4.31E-02
9	Signal Transduction_BMP and GDF signaling	5.81E-02
10	Immune_Antigen presentation	6.05E-02

lyzed via cDNA microarray to examine whether the differentially expressed miRNAs could regulate their target genes. Because the absolute standard of miRNA is not available at present, and miRNA expression was compared within the samples and genes analyzed in this study, there might be possible errors when a larger number of samples and genes were analyzed.

Using these systems, we found that the expression profile in miRNAs was clearly different according to HBV and HCV infection for the first time. The differences were confirmed by the nonsupervised learning method, hierarchical clustering (Fig. 2A), and supervised learning methods based on SVM at an 87% accuracy ($P < 0.001$) (Table 2-1). As similarly described, the expression profile in miRNAs was significantly different according to the progression of liver disease (normal, CH, and HCC) in this study. The present CH and HCC expression data were derived from the same patient, and some microarray analyses suggested that the noncancerous liver tissue can predict the prognosis of HCC.[19,20] We examined whether the miRNA expression of paired samples was similar or independent using the Dunnett test[12] (Supplementary Data). Our data indicated that miRNA expression profiling was more dependent on the disease condition than on the paired condition, although the issue of paired samples should be taken into account carefully.

Table 4-2. Pathway Analysis of Targeted Genes by Differentially Expressed miRNAs Between HBV-Related Liver Disease (CH-B,HCC-B) and HCV Related Liver Disease (CH-C,HCC-C Cluster 2)

No.	Pathway Name	*P* Value
Down-regulated miRNA in CH-C,HCC-C (possibly up-regulating target genes)		
1	Immune_Phagosome in antigen presentation	5.80E-04
2	Muscle contraction	1.05E-03
3	Immune_Antigen presentation	5.75E-03
4	Cell cycle_Meiosis	1.49E-02
5	Reproduction_Male sex differentiation	2.06E-02
6	Cell adhesion_Platelet aggregation	2.77E-02
7	Transport_Synaptic vesicle exocytosis	3.56E-02
8	Inflammation_Kallikrein-kinin system	3.73E-02
9	Inflammation_IgE signaling	4.10E-02
10	Development_Skeletal muscle development	5.02E-02
Down-regulated miRNA in CH-B,HCC-B (possibly up-regulating target genes)		
1	Signal Transduction_Cholecystokinin signaling	1.15E-04
2	Inflammation_NK cell cytotoxicity	5.29E-03
3	Signal transduction_CREM pathway	5.31E-03
4	Reproduction_GnRH signaling pathway	7.80E-03
5	DNA damage_DBS repair	1.02E-02
6	Cell cycle_G2-M	1.63E-02
7	Development_Neuromuscular junction	2.07E-02
8	Apoptosis_Apoptosis mediated by external signals	2.42E-02
9	Reproduction_FSH-beta signaling pathway	2.92E-02
10	Cell adhesion_Amyloid proteins	3.81E-02

Table 4-3. The Pathway Analysis of Targeted Genes by Differentially Expressed miRNAs Between CH and HCC (Cluster 3)

No.	Pathway Name	*P* Value
	Down-regulated miRNA in HCC (possibly up-regulating target genes)	
1	Cytoskeleton_Spindle microtubules	2.15E-03
2	Transcription_Chromatin modification	5.27E-03
3	Proteolysis_Ubiquitin-proteasomal proteolysis	6.43E-03
4	Cell adhesion_Cell-matrix interactions	7.30E-03
5	Cell cycle_Meiosis	7.83E-03
6	DNA damage_Checkpoint	1.69E-02
7	Reproduction_Progesterone signaling	1.94E-02
8	Apoptosis_Apoptotic mitochondria	3.14E-02
9	Translation_Regulation of initiation	4.22E-02
10	Signal transduction_WNT signaling	4.26E-02
	Up-regulated miRNA in HCC (possibly down-regulating target genes)	
1	Inflammation_IgE signaling	1.05E-02
2	Inflammation_Kallikrein-kinin system	2.46E-02
3	Inflammation_Innate inflammatory response	2.51E-02
4	Inflammation_Histamine signaling	4.25E-02
5	Inflammation_Neutrophil activation	4.55E-02
6	Chemotaxis	4.68E-02
7	Inflammation_IL-12,15,18 signaling	5.16E-02
8	Inflammation_NK cell cytotoxicity	7.25E-02
9	Cell cycle_G0-G1	7.53E-02
10	Inflammation_Complement system	7.72E-02

Binary tree prediction analysis and detailed assessment of hierarchical clustering revealed two types of differential miRNAs, one associated with HBV and HCV infection, the other associated with the stages of liver disease that were irrelevant to the differences in HBV and HCV infection. We found that differences in miRNA expression between liver tissues with HBV and HCV (HBV/HCV) were strongly correlated with those in miRNA between cultured cell models of HBV and HCV infection (HBV/HCV) ($r = 0.73$ $P = 0.0006$) (Fig. 5). Thus, there exist HBV- and HCV-infection–specific miRNAs that potentially regulate viral replication and host gene signaling pathways in hepatocytes.

	HBV/HCV Tissue	HBV/HCV Huh7.5
hsa-miR-20	0.61	0.36
hsa-miR-23a	-1.12	-1.3
hsa-miR-27a	-0.75	-1.51
hsa-miR-34c	-2.29	N.D.
hsa-miR-105	2.13	N.D.
hsa-miR-124b	-1.63	-10.54
hsa-miR-133b	1.28	-3.64
hsa-miR-134	2.52	-0.63
hsa-miR-142-5p	-1.34	-4.39
hsa-miR-151	0.86	-0.29
hsa-miR-182*	1.16	0.37
hsa-miR-190	1.04	1.32
hsa-miR-191	0.48	1.16
hsa-miR-193	0.74	-0.03
hsa-miR-194	0.74	0.76
hsa-miR-211	4.68	5.26
hsa-miR-324-5p	0.59	1.16
hsa-miR-340	0.57	1.68
hsa-let-7a	-1.14	-4.51

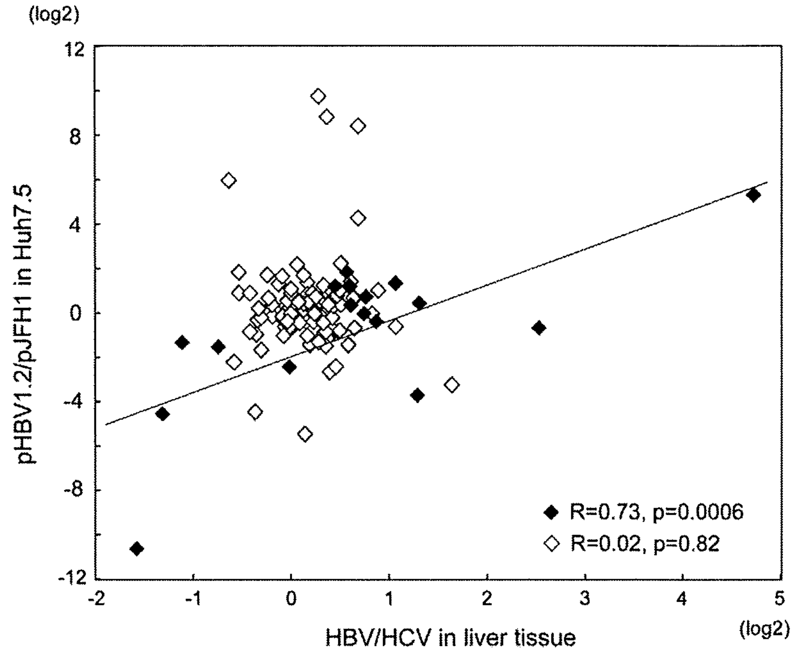

Fig. 5. Correlation between differences in miRNA expression between liver tissues infected with HBV and HCV and those in miRNA expression between cultured cell models of HBV and HCV infections. A total of 140 of 188 miRNAs were confirmed to be expressed in Huh7.5 cells. There was a significant correlation of infection-associated miRNA (closed lozenge) in vitro and in vivo (r = 0.73, P = 0.0006), but none for the other 121 miRNAs (open lozenge) (r = 0.02, P = 0.82).

The pathway analysis of targeted genes by miRNAs revealed that 13 miRNAs exhibiting a decreased expression in the HCV group regulate genes related to immune response, antigen presentation, cell cycle, proteasome, and lipid metabolism. Six miRNAs showing a decreased expression in the HBV group regulate genes related to cell death, DNA damage and recombination, and transcription signals. These findings reflected differences in the gene expression profile between CH-B and CH-C as described.[10] Many of the miRNAs were down-regulated in the HCV group rather than in the HBV group. It has been reported that human endogenous miRNAs may be involved in defense mechanisms, mainly against RNA viruses.[21] On the other hand, it is suggested that endogenous miRNAs may be consumed and reduced by defense mechanisms, especially those against RNA viruses.

Although the expressions of these HBV- and HCV-infection–specific miRNAs were irrelevant to the differences in CH and HCC (Fig. 3, cluster 2), some of them have been reported to play pivotal roles in the occurrence of cancer. For example, has-let-7a regulates ras and c-myc genes,[22] and has-miR-34 is involved in the p53 tumor suppressor pathway.[23] These miRNAs were down-regulated in the HBV group, possibly participating in a more aggressive and malignant phenotype in HCC-B rather than in HCC-C. High expression of has-miR-191 was shown to be significantly associated with the worse survival in acute myeloid leukemia,[24] and has-miR-191 was overexpressed in the HBV group compared with the HCV group. On the other hand, has-miR-133b, which was reported to be down-regulated in squamous cell carcinoma,[25] was repressed in the HCV group compared with the HBV group. Some hematopoietic-specific miRNAs such as has-miR-142-5p were up-regulated in the HCV group. Therefore, these miRNAs were not only HBV and HCV infection–associated but also tumor-associated. These findings indicate different mechanisms of development of HCC infected with HBV and HCV (Fig. 6).

Following HCC development, common changes in miRNA expression between HCC-B and HCC-C appeared (Fig. 3, cluster 3). The 23 miRNAs mentioned above clearly differentiated CH and HCC that were irrelevant to the differences in HBV and HCV infections. Seventeen miRNAs were down-regulated in HCC, which up-regulated cancer-associated pathways. Six miRNAs were up-regulated in HCC that down-regulated all inflammation-mediated signaling pathways, potentially reflecting impaired antitumor immune response in HCC. These results suggest that common signaling pathways are involved in HCC development from CH, and that HBV- and HCV-specific miRNAs participate in generating HCC-specific miRNA expressions (Fig. 6). Therefore, these miRNAs might be good candidates for molecular targeting to prevent HCC occurrence, because they reg-

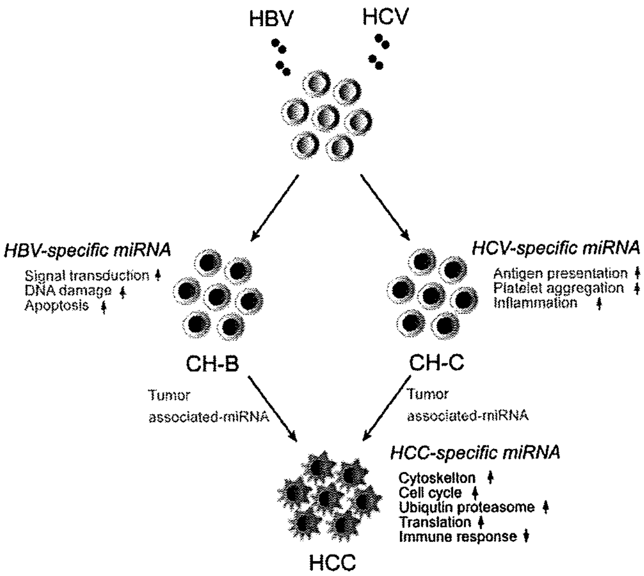

Fig. 6. Infection-associated and HCC-specific miRNAs and liver disease progression.

ulate a common signaling pathway underlying HCC-B and HCC-C development.

In conclusion, we showed that miRNAs are important mediators of HBV and HCV infections as well as liver disease progression. Further studies are needed to enable more detailed mechanistic analysis of the miRNAs identified here and to evaluate the usefulness of miRNAs as diagnostic/prognostic markers and potential therapeutic target molecules.

Acknowledgement: The authors thank Mikiko Nakamura and Nami Nishiyama for excellent technical assistance.

References

1. He L, Thomson JM, Hemann MT, Hernando-Monge E, Mu D, Goodson S, et al. A microRNA polycistron as a potential human oncogene. Nature 2005;435:828-833.
2. Calin GA, Dumitru CD, Shimizu M, Bichi R, Zupo S, Noch E, et al. Frequent deletions and down-regulation of micro-RNA genes miR15 and miR16 at 13q14 in chronic lymphocytic leukemia. Proc Natl Acad Sci U S A 2002;99:15524-15529.
3. Cho WC. OncomiRs: the discovery and progress of microRNAs in cancers. Mol Cancer 2007;6:60.
4. Hutvagner G, Zamore PD. A microRNA in a multiple-turnover RNAi enzyme complex. Science 2002;297:2056-2060.
5. Ambros V, Bartel B, Bartel DP, Burge CB, Carrington JC, Chen X, et al. A uniform system for microRNA annotation. RNA 2003;9:277-279.
6. Lee RC, Feinbaum RL, Ambros V. The C. elegans heterochronic gene lin-4 encodes small RNAs with antisense complementarity to lin-14. Cell 1993;75:843-854.
7. Lewis BP, Burge CB, Bartel DP. Conserved seed pairing, often flanked by adenosines, indicates that thousands of human genes are microRNA targets. Cell 2005;120:15-20.
8. Kiyosawa K, Sodeyama T, Tanaka E, Gibo Y, Yoshizawa K, Nakano Y, et al. Interrelationship of blood transfusion, non-A, non-B hepatitis and hepatocellular carcinoma: analysis by detection of antibody to hepatitis C virus. HEPATOLOGY 1990;12:671-675.
9. Honda M, Kaneko S, Kawai H, Shirota Y, Kobayashi K. Differential gene expression between chronic hepatitis B and C hepatic lesion. Gastroenterology 2001;120:955-966.
10. Honda M, Yamashita T, Ueda T, Takatori H, Nishino R, Kaneko S. Different signaling pathways in the livers of patients with chronic hepatitis B or chronic hepatitis C. HEPATOLOGY 2006;44:1122-1138.
11. Molinaro AM, Simon R, Pfeiffer RM. Prediction error estimation: a comparison of resampling methods. Bioinformatics 2005;21:3301-3307.
12. Dunnett CW. A multiple comparison procedure for comparing several treatments with a control. J Am Stat Assoc 1955;50:1096-1121.
13. Weiss L, Kekule AS, Jakubowski U, Burgelt E, Hofschneider PH. The HBV-producing cell line HepG2–4A5: a new in vitro system for studying the regulation of HBV replication and for screening anti-hepatitis B virus drugs. Virology 1996;216:214-218.
14. Lindenbach BD, Evans MJ, Syder AJ, Wolk B, Tellinghuisen TL, Liu CC, et al. Complete replication of hepatitis C virus in cell culture. Science 2005;309:623-626.
15. Wakita T, Pietschmann T, Kato T, Date T, Miyamoto M, Zhao Z, et al. Production of infectious hepatitis C virus in tissue culture from a cloned viral genome. Nat Med 2005;11:791-796.
16. Murakami Y, Yasuda T, Saigo K, Urashima T, Toyoda H, Okanoue T, et al. Comprehensive analysis of microRNA expression patterns in hepatocellular carcinoma and non-tumorous tissues. Oncogene 2006;25:2537-2545.
17. Varnholt H, Drebber U, Schulze F, Wedemeyer I, Schirmacher P, Dienes HP, et al. MicroRNA gene expression profile of hepatitis C virus-associated hepatocellular carcinoma. HEPATOLOGY 2008;47:1223-1232.
18. Budhu A, Jia HL, Forgues M, Liu CG, Goldstein D, Lam A, et al. Identification of metastasis-related microRNAs in hepatocellular carcinoma. HEPATOLOGY 2008;47:897-907.
19. Budhu A, Forgues M, Ye QH, Jia HL, He P, Zanetti KA, et al. Prediction of venous metastases, recurrence, and prognosis in hepatocellular carcinoma based on a unique immune response signature of the liver microenvironment. Cancer Cell 2006;10:99-111.
20. Hoshida Y, Villanueva A, Kobayashi M, Peix J, Chiang DY, Camargo A, et al. Gene expression in fixed tissues and outcome in hepatocellular carcinoma. N Engl J Med 2008;359:1995-2004.
21. Jopling CL, Yi M, Lancaster AM, Lemon SM, Sarnow P. Modulation of hepatitis C virus RNA abundance by a liver-specific MicroRNA. Science 2005;309:1577-1581.
22. Johnson CD, Esquela-Kerscher A, Stefani G, Byrom M, Kelnar K, Ovcharenko D, et al. The let-7 microRNA represses cell proliferation pathways in human cells. Cancer Res 2007;67:7713-7722.
23. He X, He L, Hannon GJ. The guardian's little helper: microRNAs in the p53 tumor suppressor network. Cancer Res 2007;67:11099-11101.
24. Garzon R, Volinia S, Liu CG, Fernandez-Cymering C, Palumbo T, Pichiorri F, et al. MicroRNA signatures associated with cytogenetics and prognosis in acute myeloid leukemia. Blood 2008;111:3183-3189.
25. Wong TS, Liu XB, Chung-Wai Ho A, Po-Wing Yuen A, Wai-Man Ng R, Ignace Wei W. Identification of pyruvate kinase type M2 as potential oncoprotein in squamous cell carcinoma of tongue through microRNA profiling. Int J Cancer 2008;123:251-257.

ELSEVIER

Journal of Hepatology 50 (2009) 100–110

Journal of Hepatology

www.elsevier.com/locate/jhep

Activation of lipogenic pathway correlates with cell proliferation and poor prognosis in hepatocellular carcinoma☆

Taro Yamashita[1], Masao Honda[1,2], Hajime Takatori[1], Ryuhei Nishino[1], Hiroshi Minato[3], Hiroyuki Takamura[4], Tetsuo Ohta[4], Shuichi Kaneko[1,*]

[1]*Department of Gastroenterology, Kanazawa University Graduate School of Medical Science, 13-1 Takara-Machi, Kanazawa 920-8641, Japan*
[2]*Department of Advanced Medical Technology, Kanazawa University School of Health Sciences, 13-1 Takara-Machi, Kanazawa 920-8641, Japan*
[3]*Pathology Section, Kanazawa University Hospital, 13-1 Takara-Machi, Kanazawa 920-8641, Japan*
[4]*Department of Gastroenterologic Surgery, Kanazawa University Graduate School of Medical Science, 13-1 Takara-Machi, Kanazawa 920-8641, Japan*

***Background/Aims*: Metabolic dysregulation is one of the risk factors for the development of hepatocellular carcinoma (HCC). We investigated the activated metabolic pathway in HCC to identify its role in HCC growth and mortality.**

***Methods*: Gene expression profiles of HCC tissues and non-cancerous liver tissues were obtained by serial analysis of gene expression. Pathway analysis was performed to characterize the metabolic pathway activated in HCC. Suppression of the activated pathway by RNA interference was used to evaluate its role in HCC *in vitro*. Relation of the pathway activation and prognosis was statistically examined.**

***Results*: A total of 289 transcripts were up- or down-regulated in HCC compared with non-cancerous liver ($P < 0.005$). Pathway analysis revealed that the lipogenic pathway regulated by sterol regulatory element binding factor 1 (*SREBF1*) was activated in HCC, which was validated by real-time RT-PCR. Suppression of *SREBF1* induced growth arrest and apoptosis whereas overexpression of *SREBF1* enhanced cell proliferation in human HCC cell lines. *SREBF1* protein expression was evaluated in 54 HCC samples by immunohistochemistry, and Kaplan–Meier survival analysis indicated that *SREBF1*-high HCC correlated with high mortality.**

***Conclusions*: The lipogenic pathway is activated in a subset of HCC and contributes to cell proliferation and prognosis.**

***Keywords*: Hepatocellular carcinoma; Serial analysis of gene expression; Lipogenesis; Gene expression profiling; Sterol regvulatory element binding factor 1**

Received 26 May 2008; received in revised form 1 July 2008; accepted 23 July 2008; available online 12 October 2008
Associate Editor: J.M. Llovet

☆ The authors who have taken part in the research of this paper declared that they do not have a relationship with the manufacturers of the materials involved either in the past or present and they did not receive funding from the manufacturers to carry out their research.

* Corresponding author. Tel.: +81 76 265 2231; fax: +81 76 234 4250.
E-mail address: skaneko@m-kanazawa.jp (S. Kaneko).

Abbreviations: HCC, hepatocellular carcinoma; *SREBF1*, sterol regulatory element binding factor 1; HBV, hepatitis B virus; HCV, hepatitis C virus; SAGE, serial analysis of gene expression; RT-PCR, reverse transcription-polymerase chain reaction; IHC, immunohistochemistry; FADS1, fatty acid desaturase 1; SCD, stearoyl CoA desaturase; FASN, fatty acid synthase; si-RNA, short interfering-RNA; CLD, chronic liver disease; PCNA, proliferating cell nuclear antigen; IGF, insulin-like growth factor.

1. Introduction

Hepatocellular carcinoma (HCC) is one of the most frequently occurring malignancies in the world [1]. The major risk factors associated with HCC include chronic infection with hepatitis B virus (HBV) and hepatitis C virus (HCV), alcohol abuse, and exposure to aflatoxin B1 [2]. HCC usually develops from liver cirrhosis, which involves continuous inflammation and hepatocyte regeneration, suggesting that reactive oxygen species and DNA damage are involved in the process of hepatocarcinogenesis [3].

The development of gene expression profiling technologies including DNA microarrays and serial analysis

0168-8278/$34.00 © 2008 European Association for the Study of the Liver. Published by Elsevier B.V. All rights reserved.
doi:10.1016/j.jhep.2008.07.036

of gene expression (SAGE) have enhanced our ability to identify inventory transcripts and global genetic alterations in HCC [4–10]. In general, these methods have demonstrated that transcripts associated with cell growth are up-regulated, whereas those related to inhibition of cell growth are down-regulated, in HCC [11]. It is difficult, however, to decipher molecular pathways activated during hepatocarcinogenesis.

Epidemiological studies suggest that metabolic dysregulation in the liver increases the risk of HCC development. For example, diabetes is associated with a 2-fold increase in the risk of HCC [12]. Obesity and hepatic steatosis also increase the risk of HCC [13–15]. Furthermore, recent studies indicate that HCV infection provokes hepatic steatosis, which may be a vulnerable factor for liver inflammation and HCC development [16,17]. Thus, dysregulation of a metabolic pathway may play a crucial role to promote HCC growth, but the molecular mechanism is still obscure. In this study, we have utilized SAGE [18,19], which enables us to monitor the differential expression of all genes, to determine the global changes in gene expression that occur during hepatocarcinogenesis.

2. Materials and methods

2.1. Tissue samples

All HCC tissues, adjacent non-cancerous liver tissues, and normal liver tissues were obtained from 69 patients who underwent hepatectomy from 1997 to 2005 in Kanazawa University Hospital. Normal liver tissue samples were obtained from patients undergoing surgical resection of the liver for treatment of metastatic colon cancer. HCC and surrounding non-cancerous liver samples were obtained from patients undergoing surgical resection of the liver for the treatment of HCC. The samples used for SAGE, real-time reverse-transcription (RT)-PCR analysis, and immunohistochemistry (IHC) are listed in Supplemental Table 1. All samples used for SAGE and real-time RT-PCR analysis were snap-frozen in liquid nitrogen. Four normal liver tissues and 20 HCCs and their corresponding non-cancerous liver tissues were used for real-time RT-PCR analysis; seven of these HCC samples, along with 47 additional HCC samples, were formalin-fixed paraffin-embedded and used for IHC. HCC and adjacent non-cancerous liver were histologically characterized as described [20].

All strategies used for gene expression analysis as well as tissue acquisition processes were approved by the Ethics Committee and the Institutional Review Board of Kanazawa University Hospital. All procedures and risks were explained verbally, and each patient provided written informed consent.

2.2. SAGE

Total RNA was purified from each homogenized tissue sample using a ToTally RNA extraction kit (Ambion, Inc., Austin, TX), and polyadenylated RNA was isolated using a MicroPoly (A) Pure kit (Ambion). A total of 2.5 μg mRNA per sample was analyzed by SAGE [18]. SAGE libraries were randomly sequenced at the Genomic Research Center (Shimadzu-Biotechnology, Kyoto, Japan), and the sequence files were analyzed with SAGE 2000 software. The size of each SAGE library was normalized to 300,000 transcripts per library, and the abundance of transcripts was compared by SAGE 2000 software. Monte Carlo simulation was used to select genes with significant differences in expression between two libraries without multiple hypothesis testing correction ($P < 0.005$) [21]. Each SAGE tag was annotated using a gene-mapping web site (http://www.ncbi.nlm.nih.gov/SAGE/index.cgi).

2.3. Analysis of signaling networks

Ingenuity Pathways Analysis software (Ingenuity® Systems, www.ingenuity.com) was used to investigate the molecular pathways activated in an HCC SAGE library compared with an adjacent non-cancerous liver SAGE library. All reliable transcripts statistically up-regulated in HCC were investigated and annotated with biological processes, protein-protein interactions, and gene regulatory networks, using a reference-based data file with statistical significance. All identified pathways were screened individually. MetaCore™ software (GeneGo Inc., St. Joseph, MI) was used to evaluate candidate transcription factors responsible for up-regulation of transcripts in HCC.

2.4. RT-PCR

A 1-μg aliquot of each total RNA was reverse-transcribed using SuperScript II reverse-transcriptase (Invitrogen, Carlsbad, CA). Real-time RT-PCR analysis was performed using ABI PRISM 7900 Sequence Detection System (Applied Biosystems, Foster City, CA). Using the standard curve method, quantitative **PCR** was performed in triplicate for each sample-primer set. Each sample was normalized relative to β-actin. The assay IDs used were Hs00231674_m1 for sterol regulatory element binding factor 1 (*SREBF1*); Hs00203685_m1 for fatty acid desaturase 1 (*FADS1*) ;Hs00748952_s1 for stearoyl CoA desaturase (*SCD*); Hs001 88012_m1 for fatty acid synthase (*FASN*); and Hs99999_m1 for β-actin. *SREBF1a* and *SREBF1c* mRNA levels were assayed by semi-quantitative RT-PCR [22].

2.5. RNA Interference targeting SREBF1

Si-RNAs targeting *SREBF1* were constructed using a *Silencer*™ SiRNA Construction kit (Ambion) according to the manufacturer's protocol. We constructed two different si-RNAs, targeting different sites of *SREBF1* (*SREBF1*-1; CAGTGGCACTGACTCTTCC, *SREBF1*-2; TCTACGACCAGTGGGACTG). Control si-RNA duplexes targeting scramble sequences were also synthesized (Dharmacon Research, Inc., Lafayette, CO). Lipofectamine 2000™ reagent (Invitrogen) was used for transfection according to the manufacturer's instructions.

2.6. Cell proliferation assay

Cell proliferation assays were performed using a Cell Titer96 Aqueous kit (Promega, Madison, WI). Results are expressed as the mean optical density (OD) of each five-well set. All experiments were repeated at least twice.

2.7. Soft agar assay

To each well of a six-well plate, containing a base layer of 0.72% agar in growth medium, was added 1×10^4 cells, suspended in 2 ml of 0.36% agar with growth medium (DMEM supplemented with 10% FBS), and the plates were incubated at 37 °C in a 5% CO_2 incubator for 2 weeks. The numbers of colonies in each well were counted as previously described [23].

2.8. TUNEL assay

A DeadEnd™ Colorimetric TUNEL System (Promega) was used to measure nuclear DNA fragmentation as described previously [24].

2.9. Annexin V staining

To evaluate apoptotic cell death, Annexin V binding to cell membranes was evaluated using Annexin V-FITC antibodies and FACSCalibur flow cytometer (BD Biosciences, Franklin Lakes, NJ), as described by the manufacturer.

2.10. Focus assay

HuH7 cells and Hep3B cells were transiently transfected with pCMV7 or pCMV7-*SREBF1c* vectors (kindly provided by Dr. Hitoshi Shimano) using Lipofectamine 2000^{TM} reagent (Invitrogen), as described by the manufacturer. A total of 2×10^3 cells were seeded on six-well plates 48 h after transfection, and cultured in usual media with 400 ng/ml of Geneticin for 9 days. The foci were fixed with ice-cold 100% methanol and stained with 0.5% crystal violet solution. All experiments were performed in triplicates.

2.11. Western blotting

Whole cell lysates were prepared using RIPA lysis buffer. Antibodies used were rabbit polyclonal antibodies to phospho-GSK-3β (ser9) (Cell Signaling Technology Inc., Danvers, MA), rabbit anti-sterol regulatory element binding protein-1 (encoded by *SREBF1)* polyclonal antibody H-160 (Santa Cruz Biotechnology, Inc., Santa Cruz, CA), and β-actin (Sigma–Aldrich Japan K.K., Tokyo, Japan). Immune complexes were visualized by enhanced chemiluminescence (Amersham Biosciences Corp., Piscataway, NJ) as described in the manufacturer's protocol.

2.12. Immunohistochemistry

Rabbit anti-*SREBF1* polyclonal antibody H-160 (Santa Cruz Biotechnology, Inc.) and mouse anti-proliferating cell nuclear antigen (PCNA) monoclonal antibody PC10 (Calbiochem, San Diego, CA) were used to evaluate the immunoreactivity of HCC samples, using a DAKO EnVision+^{TM} Kit, as described by the manufacturer. The signal intensity of *SREBF1* was scored as negative, low, or high determined by the representative staining of the normal liver tissue and cirrhotic liver tissue (Supplemental Fig. 1). HCC was referred as *SREBF1*-high if *SREBF1* expression in the tumor was higher than that in the cirrhotic liver tissue. PCNA index was evaluated as previously described [25].

2.13. Statistical analysis

Kruskal–Wallis test was used to compare the differentially expressed genes, as shown by real-time PCR, among normal liver, CLD, and HCC tissues. Mann–Whitney U test was also used to evaluate the statistical significance of differences of gene expression between CLD and HCC tissues. Spearman's correlation coefficient was used to assess correlations between the expression levels of *SREBF1*, *FADS1*, *SCD*, and *FASN*. Univariate Cox proportional hazards regression analysis was used to evaluate the association of gene expression and clinicopathologic parameters with patient outcomes. All statistical analyses were performed using SPSS software (SPSS software package; SPSS Inc., Chicago, IL) and GraphPad Prism software (GraphPad Software Inc., La Jolla, CA).

3. Results

3.1. Gene expression profiling of HCC

We constructed two SAGE libraries from a HCC–HBV tissue and a corresponding non-cancerous tissue (chronic liver disease (CLD)–HBV). We also used two previously described SAGE libraries, from an HCC–HCV sample and a corresponding non-cancerous tissue sample (CLD–HCV) [4]. After excluding tags detected only once in each library, to avoid the contamination of tags derived from sequence errors, we selected 105,288 tags corresponding to the 9731 genes in all libraries. Using Monte Carlo simulation, we compared the differentially expressed transcripts in HCC and corresponding CLD libraries. Compared with their corresponding CLD libraries, there were statistically significant increases or decreases in 140 transcripts in the HCC–HBV library and in 197 transcripts in the HCC–HCV library ($P < 0.005$).

The HCC–HBV library contained one SAGE tag encoding the HBV–X region, which was increased more than 35-fold compared with its expression in the corresponding CLD–HBV library (Supplemental Table 2). We identified two additional SAGE tags, encoding unknown genes (GTTCTAAAGG, GCATTATGAT), which were expressed more than 10-fold in the HCC–HBV library than in the corresponding CLD–HBV library. The HCC–HBV library also contained tags associated with lipogenesis, at greater than 10-fold abundance, in the HCC–HBV library; these including tags for steroyl-CoA desaturase, fatty acid synthase, and fatty acid desaturase 1.

In contrast, SAGE tags associated with the immune response were up-regulated in the HCC–HCV library. These included tags for Th1-type chemokines, including chemokine ligand 10 (C–X–C motif), chemokine ligand 9 (C–X–C motif), and major histocompatibility complex classes IA and IB (Supplemental Table 3). In addition, tags associated with lipogenesis were increased in the HCC–HCV library, including tags for 3-hydroxy-3-methylglutaryl-coenzyme A synthase 1 and cytochrome P450, family 51, subfamily A, polypeptide 1. Taken together, the differential gene expression patterns may exist in HCC–HBV and HCC–HCV. HBV–X and lipogenesis-related genes are activated in HCC–HBV, whereas genes associated with inflammation as well as lipogenesis are activated in HCC–HCV.

3.2. Analysis of molecular pathways activated in HCC

To further characterize the gene expression patterns of HCC–HBV and HCC–HCV, we performed pathway analysis on SAGE data. Using MetaCore^{TM} software, we found that the candidate transcription factors activated were distinct in each HCC library (Table 1). Several of these transcription factors, including NF-κB, c-Myc, c-Jun, and HNF4-α, have been reported to be activated in HCC [26–29]. In addition, our findings indicated that the transcription factor *SREBF1* may be activated in both HCC–HBV and HCC–HCV (to avoid a confusion, we use HUGO symbol *SREBF1* to indicate both gene/protein name).

Table 1
Candidate transcription factors that regulate molecular pathways activated in HCC.

SAGE library	Transcription factor	Molecular processes	*P*-value
HCC–HCV	NF-κB	Antigen presentation Antigen processing Defense response Immune response	0.004
	SREBF1	Cholesterol biosynthesis Lipid biosynthesis β-Glucoside transport Negative regulation of lipoprotein metabolism	0.05
	SP1	Electron transport; drug metabolism Oxygen and reactive oxygen species metabolism Cell-substrate junction assembly; wound healing	0.05
	IRF1	Immune response Antigen presentation; antigen processing Defense response; positive regulation of cell	0.05
HCC–HBV	HNF4-α	Lipid transport Fatty acid metabolism Smooth muscle cell proliferation	0.002
	HNF1	Acute-phase response; lipid transport Negative regulation of lipid catabolism β-Glucoside transport Negative regulation of lipoprotein metabolism	0.01
	SP1	Zinc ion homeostasis; response to biotic stimulus Nitric oxide mediated signal transduction Copper ion homeostasis; fatty acid biosynthesis	0.01
	c-Jun	Progesterone catabolism; progesterone metabolism Regulation of lipid metabolism; Prostaglandin metabolism	0.03
	C/EBP-α	Lipid transport; negative regulation of lipid catabolism Negative regulation of lipoprotein metabolism β-Glucoside transport Positive regulation of interleukin-8 biosynthesis	0.03
	SREBF1	Lipid biosynthesis; fatty acid biosynthesis Fatty acid metabolism Negative regulation of lipid catabolism Negative regulation of lipoprotein metabolism	0.03
	c-Myc	Fatty acid biosynthesis; fatty acid metabolism Fatty acid desaturation; Activation of pro-apoptotic gene products Release of cytochrome c from mitochondria	0.03
	USF1	Fatty acid metabolism Smooth muscle cell proliferation	0.03
	PPAR-α	Fatty acid metabolism Smooth muscle cell proliferation	0.03
	COUP-TFI	Lipid transport Smooth muscle cell proliferation	0.03
	C/EBP-β	Acute-phase response Regulation of interleukin-6 biosynthesis Fat cell differentiation Inflammatory response	0.03

These findings were evaluated by other pathway analysis software, Ingenuity Pathways Analysis (IPA). We applied the signaling network analysis to the transcripts up-regulated in the HCC libraries ($P < 0.005$). We found that the top signaling network activated in HCC–HBV contained several pathways involved in ERK/MAPK signaling, PPAR signaling, linoleic acid metabolism, and fatty acid metabolism (Supplemental Fig. 2A). Similarly, pathways involved in interferon signaling, NF-κB signaling, antigen presentation, PPAR signaling, linoleic acid metabolism, and fatty acid metabolism were included in the top signaling network activated in HCC–HCV (Supplemental Fig. 2B). Consistent with the results of transcription factor analysis by MetaCore™, pathway analysis indicated that *SREBF1* participates in the lipogenesis pathway in both HCC–HBV and HCC–HCV (blue nodes in Supplemental Fig. 2A and B). *SREBF1*, a major regulator of the lipogenesis pathway, binds to sterol regulatory elements on the genome [30], but less is known about its role in

HCC [31]. We therefore focused on the role of *SREBF1* signaling in HCC.

3.3. Validation of SAGE and signaling network analysis

We performed real-time RT-PCR analysis of *SREBF1* and three representative target genes (*SCD*, *FADS1*, and *FASN*) [20] on 44 samples not used for SAGE. We found that the levels of *SREBF1, SCD*, and *FASN* mRNAs were higher in HCC tissues and CLD tissues compared with normal liver, and that these differences were statistically significant (Fig. 1A). We further compared the expression of *SREBF1*, *FADS1*, and *FASN* between HCC and non-cancerous liver tissues, and identified the overexpression of *SREBF1* in HCC with statistical significance (Supplemental Fig. 3). Scatter plot analysis showed that the expression levels of *SREBF1* were correlated with those of *FADS1* ($R = 0.57$, $P < 0.0001$), *SCD* ($R = 0.82$, $P < 0.0001$), and *FASN* ($R = 0.74$, $P < 0.0001$) (Fig. 1B).

Since the mammalian genome encodes two *SREBF1* isoforms, *SREBF1a* and *SREBF1c* [22], we performed semi-quantitative RT-PCR with isoform specific primers to determine which of these isoforms was up-regulated in HCC. We found that *SREBF1c* mRNA, but not *SREBF1a* mRNA, was up-regulated in HCC compared with adjacent non-cancerous liver and normal liver tissues (Supplemental Fig. 4A).

3.4. Functional assay of the lipogenesis pathway in cell lines

Although genome-wide expression profiling showed that the lipogenesis pathway was activated in HCC possibly through up-regulation of *SREBF1*, it was not clear that this pathway played a role in HCC growth. To investigate the role of lipogenesis in HCC cell proliferation, we transfected two short interfering (si)-RNAs (*SREBF1*-1 and *SREBF1*-2) targeting *SREBF1* into the HuH7 and Hep3B cells. These cell lines have no chromosome amplification or deletion on 17p11, on which *SREBF1* is located [32]. Transfection of the si-RNA constructs for *SREBF1*-1 or *SREBF1*-2 decreased expression of *SREBF1* 90% and 70%, respectively, and the expression of both *SCD* and *FADS1* 70% and 60%, respectively (Fig. 2A). Because differences in *SREBF1c* and *SREBF1a* *sequence alignments* are very small, we could not design si-RNAs specifically targeting *SREBF1c*. We therefore checked the effect of si-RNAs on the expression of the *SREBF1* isoforms. We found that the expression of *SREBF1c* was relatively more suppressed than that of *SREBF1a* (Supplemental Fig. 4B), which may have been associated with the higher expression of *SREBF1a* than *SREBF1c* in cultured cell lines [25].

We found that the growth of these transfected cells was significantly inhibited at 72 h compared with mock transfected cells (Fig. 2B and Supplemental Fig.5A). Examination of anchorage independent cell growth showed strong suppression by deactivation of the lipogenesis pathway (Fig. 2C). Because insulin-like growth factor (IGF) is known to induce cancer cell proliferation through activation of PI3-kinase signaling followed by *SREBF1* induction, we investigated the effect of *SREBF1* knockdown on IGF2 mediated cell proliferation. Interestingly, *SREBF1* knockdown abrogated the IGF2 dependent cell proliferation (Supplemental Fig. 5B). Moreover, both the TUNEL assay and annexin V staining showed that transfection of *SREBF1* si-RNAs increased apoptosis compared with mock transfected cells (Fig. 2D and E).

We further investigated the role of *SREBF1* overexpression on cell growth *in vitro*. We transiently transfected control pCMV7 plasmids or pCMV7-*SREBF1c* plasmids (Fig. 3A), and cell proliferation was enhanced in *SREBF1* overexpressing cells compared with the control in both HuH7 and Hep3B cells evaluated by focus assay (Fig. 3B and supplemental Fig. 6). Furthermore, overexpression of *SREBF1* intensified the phosphorylation of GSK-3β, one of the major kinase phosphorylated by the activation of IGF signaling, in a dose-dependent manner (Fig. 3C).

3.5. SREBF1 Expression and prognosis

Since the above results indicated that *SREBF1* signaling may play an important role on tumor cell growth, we investigated the relationship between *SREBF1* expression and mortality in 54 HCC patients by IHC. When we examined the expression of *SREBF1* in HCC tissues and adjacent non-cancerous liver tissues, we identified the increase of the cytoplasmic *SREBF1* staining in a subset of HCC (Fig. 4A). We evaluated the expression of *SREBF1* in HCC and classified 4, 30, and 20 HCCs as *SREBF1*-negative, *SREBF1*-low, and *SREBF1*-high HCC, respectively (Fig. 4B and Supplemental Fig. 1). We could not detect any differences of clinico-pathological characteristics between *SREBF1*-high HCC and *SREBF1*-low/-negative HCC including histological steatosis (Supplemental Table4). Since the seven of these HCC samples were also used for real-time RT-PCR analysis, we investigated the relation of *SREBF1* RNA and protein expression (Fig. 4C). *SREBF1*RNA expression was significantly higher in *SREBF1*-high HCC than in *SREBF1*-low/-negative HCC with statistical significance ($P = 0.03$). Then we examined the cell proliferation of these HCC samples by PCNA staining. Notably, PCNA indexes were significantly higher in *SREBF1*-high HCC than *SREBF1*-low/-negative HCC with statistical significance ($P < 0.001$) (Fig. 4D). We further investigated the relationship between *SREBF1*

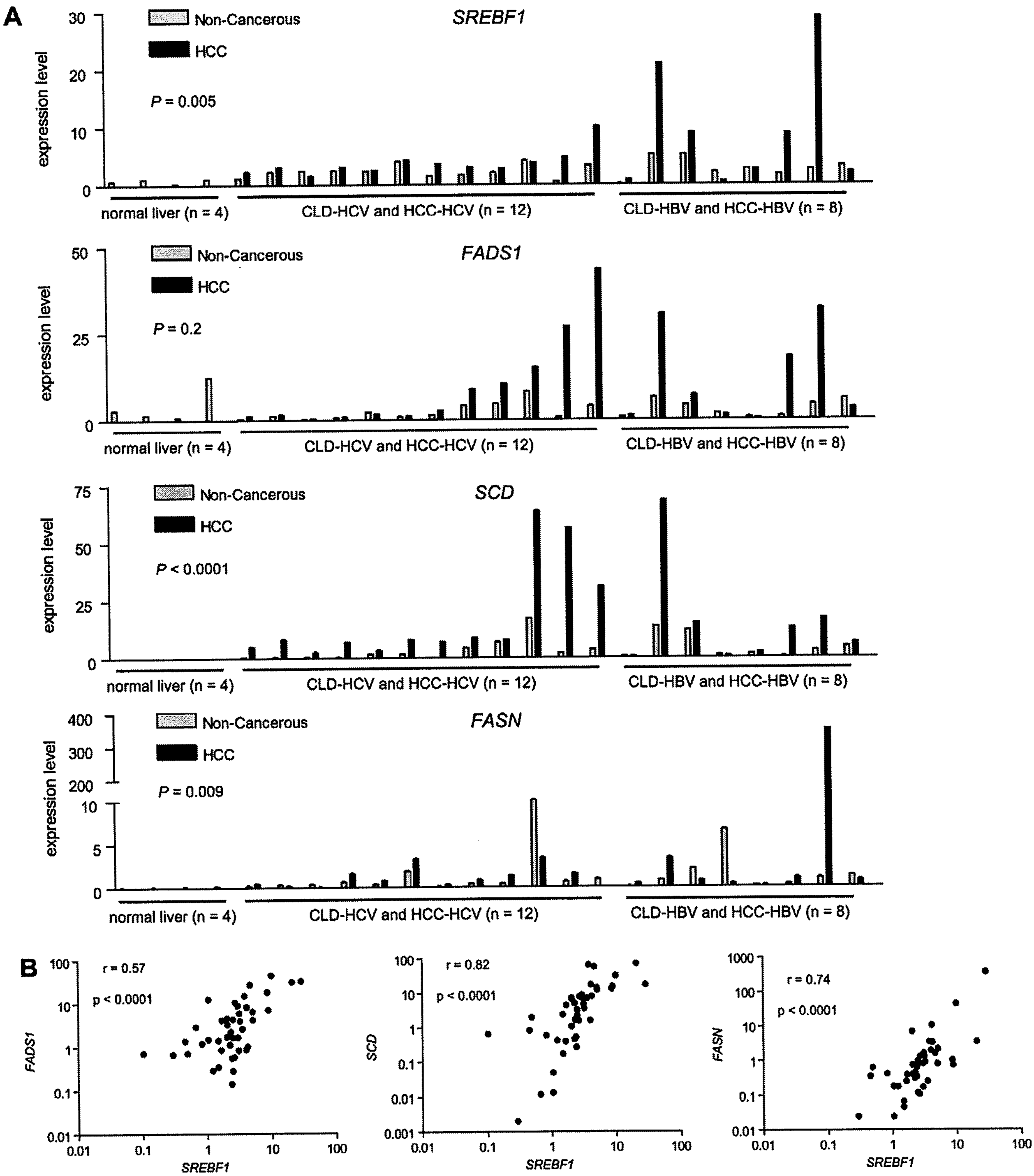

Fig. 1. (A) Real-time quantitative RT-PCR analysis. RNA was isolated from 44 tissue samples: 20 HCC, 20 corresponding CLD, and four normal liver samples. Differential expression of each gene among normal liver tissues, CLD tissues, and HCC tissues was examined by Kruskal–Wallis tests. (B) Scatter plot analysis. Gene expression levels of *FADS1*, *SCD* and *FASN* were well-correlated with those of *SREBF1*, as shown by Spearman's correlation coefficients.

protein expression and prognosis. Kaplan–Meier survival analysis showed a significant relationship between poor survival and high *SREBF1* protein expression ($P = 0.04$; Fig. 4E). Univariate Cox regression analysis showed a correlation between high *SREBF1* protein expression and high risk of mortality with statistical

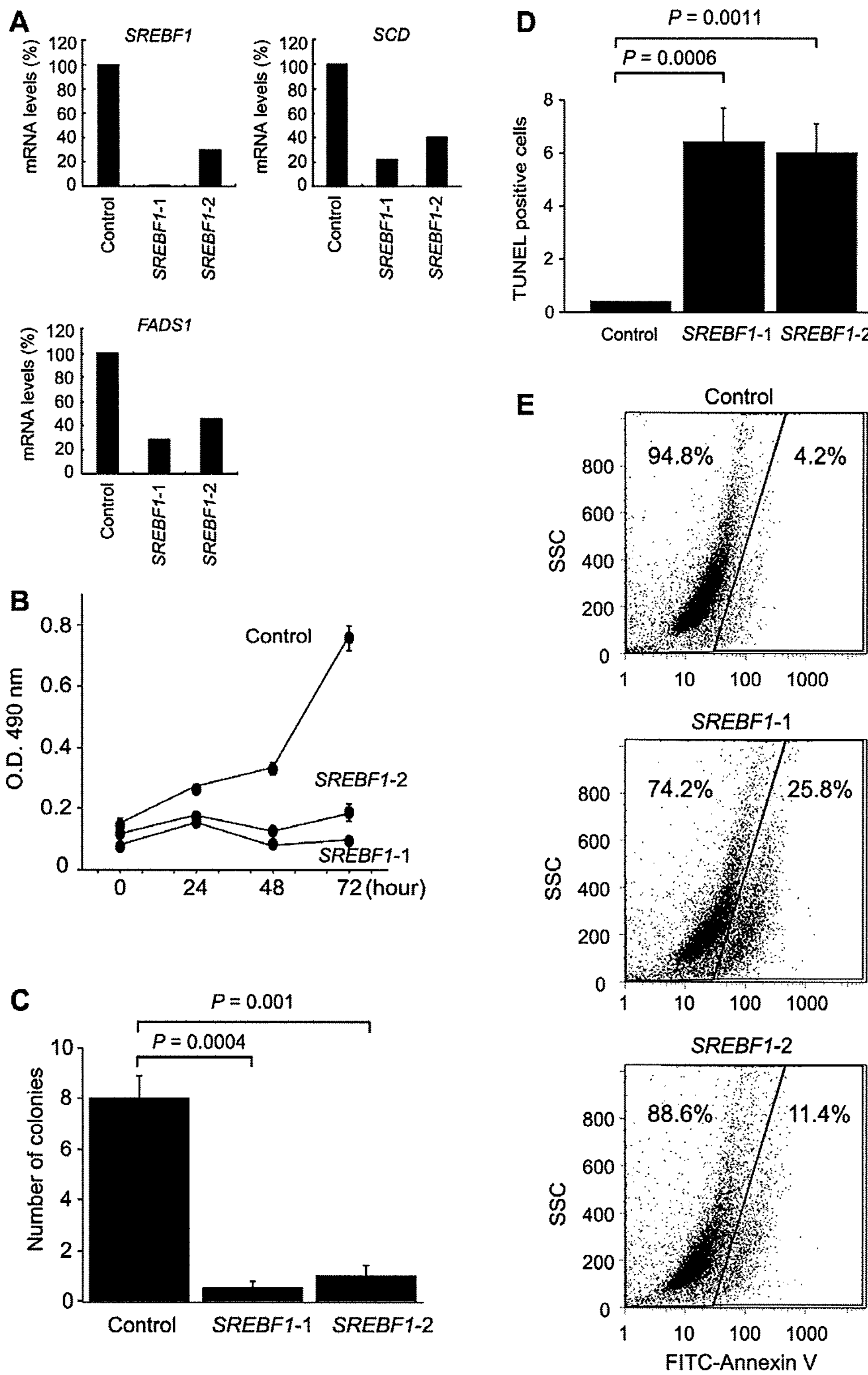

Fig. 2. (A) Effect of RNA interference targeting *SREBF1* in HuH7 cells. Expression levels of *SREBF1* mRNA were reduced by si-RNAs targeting different exons in *SREBF1*. Transcripts of *FADS1* and *SCD* were also down-regulated, showing transcriptional deactivation of the lipogenesis pathway. (B) Cell proliferation assay. Deactivation of the lipogenesis pathway severely reduced cell growth in HuH7 cells. (C) Soft agar assay. Deactivation of the lipogenesis pathway inhibited anchorage independent cell growth in HuH7 cells. (D) TUNEL assay. Deactivation of the lipogenesis pathway significantly increased the number of TUNEL-positive cells in HuH7 cells. (E) Annexin V staining evaluated by flow cytometer. Deactivation of the lipogenesis pathway significantly increased the number of annexin V positive cells in HuH7 cells.

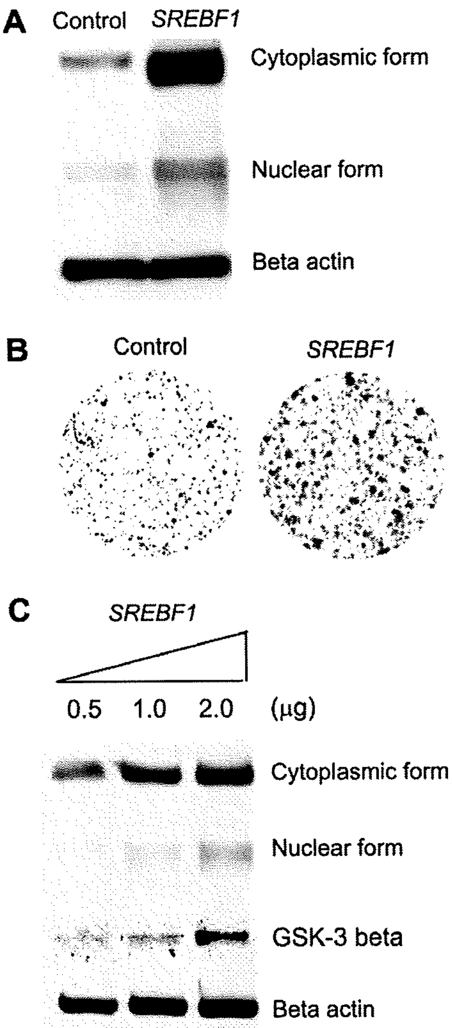

Fig. 3. (A) Western blot analysis of *SREBF1* protein expression in HuH7 cells transfected with control pCMV7 plasmids or pCMV7-*SREBF1c* plasmids. Both cytoplasmic and nuclear forms of *SREBF1* protein expression were increased by pCMV7-*SREBF1c* overexpression. (B) Focus assay of HuH7 cells transfected with control pCMV7 plasmids or pCMV7-*SREBF1c* plasmids. (C) Western blot analysis of *SREBF1* and phospho-GSK-3β protein expression in HuH7 cells transfected with indicated amounts of pCMV7-*SREBF1c* plasmids.

significance (HR, 3.7; 95% CI, 1.0–13.7; $P = 0.05$; Table 2).

4. Discussion

Using large-scale gene expression profiling, we have shown that the lipogenesis pathway is transcriptionally activated in HCC. Our SAGE profiles will be available on our homepage (http://www.intmedkanazawa.jp/) and will be submitted to the Gene Expression Omnibus (http://www.ncbi.nlm.nih.gov/geo/).

We found that the levels of expression of *FADS1*, *SCD*, and *FASN* were each correlated with those of *SREBF1*, suggesting that *SREBF1* is one of the main factors involved in the activation of lipogenesis in HCC. Activation of growth signaling pathways, such as the PI 3-kinase and mitogen-activated protein kinase pathways, has been shown to induce up-regulation of *SREBF1* in prostate and breast cancer cells [33,34]. We have observed induction of *SREBF1* protein expression by IGF2 in HuH7 cells (data not shown). Furthermore, we have identified that *SREBF1* overexpression results in the activation of cell proliferation and PI 3-kinase signaling, whereas expression inhibition of *SREBF1* abrogated the IGF2 induced cell proliferation. Although detailed mechanisms should be clarified in future, our results suggest that *SREBF1* is a key component of PI 3-kinase signaling in HCC.

SREBF1 is induced by alcohol [35], insulin, and fat [30,36], and plays a central role in the mechanism of hepatic steatosis [37]. Interestingly, these *SREBF1* inducers are risk factors for HCC [12,13,38,14]. Strikingly, two recent studies have shown that HBV and HCV infection may also induce hepatic steatosis through activation of *SREBF1* [39,40]. Furthermore, a recent report revealed the activation of *SREBF1* signaling in cancer by hypoxia [41]. Thus, these pathologic conditions such as chronic viral hepatitis, alcohol abuse, obesity, diabetes, and local hypoxia may up-regulate the expression of *SREBF1*, which, in turn, may contribute to an increased risk of hepatocarcinogenesis. Transgenic mice overexpressing *SREBF1* in the liver exhibited hepatic steatosis and hepatomegaly, suggesting the role of *SREBF1* on lipid metabolism and cell proliferation. However, it should be noted that no transgenic mice overexpressing *SREBF1* have been reported to have the risk of HCC development thus far. Interestingly, a recent report indicated that HCV core transgenic mice known to develop HCC showed coordinated activation of lipogenic pathway genes and *SREBF1* [42]. Although further studies are clearly required, we speculate that the activation of *SREBF1* may contribute to promote the development of HCC in already-initiated hepatocytes but not in normal hepatocytes.

Recently, Yahagi et al. reported the activation of lipogenic enzyme related genes in HCC [31]. In that paper, the authors suggested that *SREBF1* expression was not correlated with the expression of other lipogenic genes by Northern blotting, inconsistent with our current data. One possible explanation of these discrepancies might be the different methods for quantitation of mRNA, and we believe that real-time RT-PCR method used in our study would be more accurate. In addition, we evaluated the expression of *SREBF1* and lipogenic genes using more samples (a total of 44 liver and HCC tissues) than Yahagi et al did (10 HCC tissues). Furthermore, a recent paper indicated the coordinated activation of *SREBF1* and lipogenic genes in HCC

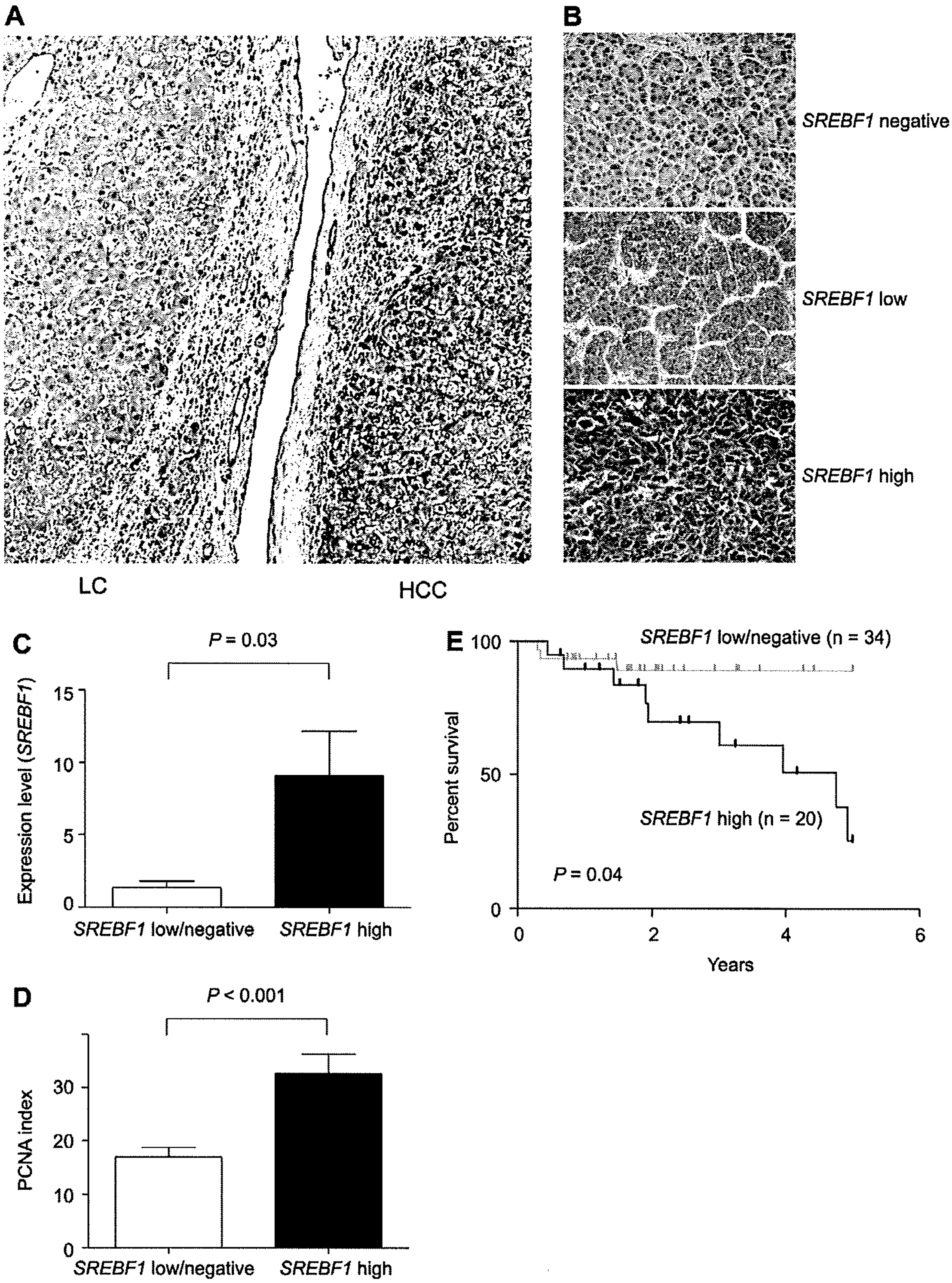

Fig. 4. (A) A photomicrograph of an HCC with adjacent non-cancerous cirrhotic liver stained with anti-*SREBF1* antibodies. (B) Representative photomicrographs of *SREBF1*-negative-, *SREBF1*-low-, and *SREBF1*-high-HCC tissues stained with anti- *SREBF1* antibodies. (C) *SREBF1* gene expression by real-time RT-PCR according to protein expression status assessed by IHC. *SREBF1* was highly expressed in *SREBF1*-high HCC ($P = 0.03$). (D) SREBF1 expression and cell proliferation in HCC. PCNA indexes in *SREBF1*-high HCC were higher than those in *SREBF1*-low/-negative HCC with statistical significance ($P < 0.001$). (E) Kaplan–Meier plots of 54 HCC patients analyzed by immunohistochemistry. The differences between *SREBF1*-high and -low/-negative HCC were analyzed by log-rank test.

developed in the liver of HCV core transgenic mice [42], strongly support our data. Although further studies using large numbers of HCC tissues may be required, these data suggest that the lipogenic gene activation seems to be mediated, at least in part, by *SREBF1* expression in HCC.

Table 2
Univariate Cox regression analysis of survival relative to *SREBF1* protein expression and clinicopathological parameters.

Variables (n)	HR (95% CI)	P-value
SREBF1 and mortality ($n = 54$)		
Tumor size		
<3 cm ($n = 37$)	1	
⩾3 cm ($n = 17$)	2.2 (0.6–8.3)	0.2
pTNM stage		
I, II ($n = 45$)	1	
III, IV ($n = 9$)	2.0 (0.4–9.4)	0.4
Serum AFP		
<20 ng/ml ($n = 35$)	1	
⩾20 ng/ml (n = 19)	1.5 (0.4–5.4)	0.5
SREBF1		
Low ($n = 34$)	1	
High ($n = 20$)	3.7 (1.0–13.7)	0.05

Because the majority of our HCC patients analyzed had Child–Pugh class A scores and about 70% had tumors less than 3 cm in diameter, all were expected to have a good prognosis. Indeed, patient survival in this cohort was not segregated by tumor size or pTNM stage (Table 2). Although the sample size was relatively small, we found that enhanced expression of *SREBF1* was a prognostic factor for mortality in HCC possibly due to the highly proliferative nature. Activation of lipogenesis pathways, as shown by overexpression of *FASN*, has been found to correlate with high mortality in breast, prostate, and lung cancer [43], suggesting that activation of lipogenesis may be a fundamental characteristic of cancer with poor prognosis. Thus, *SREBF1* expression may be a good biomarker for HCC classification, a finding that should be validated in a large scale cohort. Because deactivation of the lipogenesis pathway by inhibition of *SREBF1* gene expression could inhibit HCC cell growth *in vitro*, *SREBF1* may be a good target for pharmaceutical intervention in these tumors.

In conclusion, our genome-wide gene expression profiling analyses found that the lipogenesis pathway was activated in a subset of HCC. *SREBF1*, which activates the lipogenesis pathway, may be a good biomarker for HCC prognosis and may be a good target for therapeutic intervention.

Acknowledgements

We are grateful to the members of The Liver Disease Center at Kanazawa University Hospital for providing data of human liver tissue samples. We would also like to thank Dr. Hitoshi Shimano for providing invaluable reagents.

Appendix A. Supplementary data

Supplementary data associated with this article can be found, in the online version, at doi:10.1016/j.jhep.2008.07.036.

References

[1] El-Serag HB, Mason AC. Rising incidence of hepatocellular carcinoma in the United States. N Engl J Med 1999;340:745–750.
[2] Bosch FX, Ribes J, Diaz M, Cleries R. Primary liver cancer: worldwide incidence and trends. Gastroenterology 2004;127:S5–S16.
[3] Wang XW, Hussain SP, Huo TI, Wu CG, Forgues M, Hofseth LJ, et al. Molecular pathogenesis of human hepatocellular carcinoma. Toxicology 2002;181-182:43–47.
[4] Yamashita T, Kaneko S, Hashimoto S, Sato T, Nagai S, Toyoda N, et al. Serial analysis of gene expression in chronic hepatitis C and hepatocellular carcinoma. Biochem Biophys Res Commun 2001;282:647–654.
[5] Shirota Y, Kaneko S, Honda M, Kawai HF, Kobayashi K. Identification of differentially expressed genes in hepatocellular carcinoma with cDNA microarrays. Hepatology 2001;33:832–840.
[6] Okabe H, Satoh S, Kato T, Kitahara O, Yanagawa R, Yamaoka Y, et al. Genome-wide analysis of gene expression in human hepatocellular carcinomas using cDNA microarray: identification of genes involved in viral carcinogenesis and tumor progression. Cancer Res 2001;61:2129–2137.
[7] Xu XR, Huang J, Xu ZG, Qian BZ, Zhu ZD, Yan Q, et al. Insight into hepatocellular carcinogenesis at transcriptome level by comparing gene expression profiles of hepatocellular carcinoma with those of corresponding noncancerous liver. Proc Natl Acad Sci USA 2001;98:15089–15094.
[8] Iizuka N, Oka M, Yamada-Okabe H, Mori N, Tamesa T, Okada T, et al. Comparison of gene expression profiles between hepatitis B virus- and hepatitis C virus-infected hepatocellular carcinoma by oligonucleotide microarray data on the basis of a supervised learning method. Cancer Res 2002;62:3939–3944.
[9] Thorgeirsson SS, Grisham JW. Molecular pathogenesis of human hepatocellular carcinoma. Nat Genet 2002;31:339–346.
[10] Lee JS, Thorgeirsson SS. Genome-scale profiling of gene expression in hepatocellular carcinoma: classification, survival prediction, and identification of therapeutic targets. Gastroenterology 2004;127:S51–S55.
[11] Suriawinata A, Xu R. An update on the molecular genetics of hepatocellular carcinoma. Semin Liver Dis 2004;24:77–88.
[12] El-Serag HB, Tran T, Everhart JE. Diabetes increases the risk of chronic liver disease and hepatocellular carcinoma. Gastroenterology 2004;126:460–468.
[13] Hassan MM, Hwang LY, Hatten CJ, Swaim M, Li D, Abbruzzese JL, et al. Risk factors for hepatocellular carcinoma: synergism of alcohol with viral hepatitis and diabetes mellitus. Hepatology 2002;36:1206–1213.
[14] Ohata K, Hamasaki K, Toriyama K, Matsumoto K, Saeki A, Yanagi K, et al. Hepatic steatosis is a risk factor for hepatocellular carcinoma in patients with chronic hepatitis C virus infection. Cancer 2003;97:3036–3043.
[15] Calle EE, Rodriguez C, Walker-Thurmond K, Thun MJ. Overweight, obesity, and mortality from cancer in a prospectively studied cohort of US adults. N Engl J Med 2003;348:1625–1638.
[16] Walsh MJ, Vanags DM, Clouston AD, Richardson MM, Purdie DM, Jonsson JR, et al. Steatosis and liver cell apoptosis in chronic hepatitis C: a mechanism for increased liver injury. Hepatology 2004;39:1230–1238.

[17] Powell EE, Jonsson JR, Clouston AD. Steatosis: co-factor in other liver diseases. Hepatology 2005;42:5–13.
[18] Velculescu VE, Zhang L, Vogelstein B, Kinzler KW. Serial analysis of gene expression. Science 1995;270:484–487.
[19] Yamashita T, Hashimoto S, Kaneko S, Nagai S, Toyoda N, Suzuki T, et al. Comprehensive gene expression profile of a normal human liver. Biochem Biophys Res Commun 2000;269:110–116.
[20] Desmet VJ, Gerber M, Hoofnagle JH, Manns M, Scheuer PJ. Classification of chronic hepatitis: diagnosis, grading and staging. Hepatology 1994;19:1513–1520.
[21] Polyak K, Xia Y, Zweier JL, Kinzler KW, Vogelstein B. A model for p53-induced apoptosis. Nature 1997;389:300–305.
[22] Yokoyama C, Wang X, Briggs MR, Admon A, Wu J, Hua X, et al. SREBP-1, a basic-helix–loop-helix–leucine zipper protein that controls transcription of the low density lipoprotein receptor gene. Cell 1993;75:187–197.
[23] Wang HC, Chang WT, Chang WW, Wu HC, Huang W, Lei HY, et al. Hepatitis B virus pre-S2 mutant upregulates cyclin A expression and induces nodular proliferation of hepatocytes. Hepatology 2005;41:761–770.
[24] Takeba Y, Kumai T, Matsumoto N, Nakaya S, Tsuzuki Y, Yanagida Y, et al. Irinotecan activates p53 with its active metabolite, resulting in human hepatocellular carcinoma apoptosis. J Pharmacol Sci 2007;104:232–242.
[25] Closset J, Van de Stadt J, Delhaye M, El Nakadi I, Lambilliotte JP, Gelin M. Hepatocellular carcinoma: surgical treatment and prognostic variables in 56 patients. Hepatogastroenterology 1999;46:2914–2918.
[26] Arsura M, Cavin LG, Calvisi DF, Thorgeirsson SS, Eferl R, Ricci R, et al. Nuclear factor-kappaB and liver carcinogenesis. Cancer Lett 2005;229:157–169.
[27] Calvisi DF, Thorgeirsson SS. Molecular mechanisms of hepatocarcinogenesis in transgenic mouse models of liver cancer. Toxicol Pathol 2005;33:181–184.
[28] Eferl R, Ricci R, Kenner L, Zenz R, David JP, Rath M, et al. Liver tumor development. c-Jun antagonizes the proapoptotic activity of p53. Cell 2003;112:181–192.
[29] Xu L, Hui L, Wang S, Gong J, Jin Y, Wang Y, et al. Expression profiling suggested a regulatory role of liver-enriched transcription factors in human hepatocellular carcinoma. Cancer Res 2001;61:3176–3181.
[30] Horton JD, Goldstein JL, Brown MS. SREBPs: activators of the complete program of cholesterol and fatty acid synthesis in the liver. J Clin Invest 2002;109:1125–1131.
[31] Yahagi N, Shimano H, Hasegawa K, Ohashi K, Matsuzaka T, Najima Y, et al. Co-ordinate activation of lipogenic enzymes in hepatocellular carcinoma. Eur J Cancer 2005;41:1316–1322.
[32] Kawaguchi K, Honda M, Yamashita T, Shirota Y, Kaneko S. Differential gene alteration among hepatoma cell lines demonstrated by cDNA microarray-based comparative genomic hybridization. Biochem Biophys Res Commun 2005;329:370–380.
[33] Van de Sande T, De Schrijver E, Heyns W, Verhoeven G, Swinnen JV. Role of the phosphatidylinositol 3′-kinase/PTEN/Akt kinase pathway in the overexpression of fatty acid synthase in LNCaP prostate cancer cells. Cancer Res 2002;62:642–646.
[34] Yang YA, Han WF, Morin PJ, Chrest FJ, Pizer ES. Activation of fatty acid synthesis during neoplastic transformation: role of mitogen-activated protein kinase and phosphatidylinositol 3-kinase. Exp Cell Res 2002;279:80–90.
[35] You M, Fischer M, Deeg MA, Crabb DW. Ethanol induces fatty acid synthesis pathways by activation of sterol regulatory element-binding protein (SREBP). J Biol Chem 2002;277:29342–29347.
[36] Muller-Wieland D, Kotzka J. SREBP-1: gene regulatory key to syndrome X? Ann NY Acad Sci 2002;967:19–27.
[37] Sekiya M, Yahagi N, Matsuzaka T, Najima Y, Nakakuki M, Nagai R, et al. Polyunsaturated fatty acids ameliorate hepatic steatosis in obese mice by SREBP-1 suppression. Hepatology 2003;38:1529–1539.
[38] Marrero JA, Fontana RJ, Su GL, Conjeevaram HS, Emick DM, Lok AS. NAFLD may be a common underlying liver disease in patients with hepatocellular carcinoma in the United States. Hepatology 2002;36:1349–1354.
[39] Kim KH, Shin HJ, Kim K, Choi HM, Rhee SH, Moon HB, et al. Hepatitis B virus X protein induces hepatic steatosis via transcriptional activation of SREBP1 and PPARgamma. Gastroenterology 2007;132:1955–1967.
[40] Waris G, Felmlee DJ, Negro F, Siddiqui A. Hepatitis C virus induces proteolytic cleavage of sterol regulatory element binding proteins and stimulates their phosphorylation via oxidative stress. J Virol 2007;81:8122–8130.
[41] Furuta E, Pai SK, Zhan R, Bandyopadhyay S, Watabe M, Mo YY, et al. Fatty acid synthase gene is up-regulated by hypoxia via activation of Akt and sterol regulatory element binding protein-1. Cancer Res 2008;68:1003–1011.
[42] Tanaka N, Moriya K, Kiyosawa K, Koike K, Gonzalez FJ, Aoyama T. PPARalpha activation is essential for HCV core protein-induced hepatic steatosis and hepatocellular carcinoma in mice. J Clin Invest 2008;118:683–694.
[43] Kuhajda FP. Fatty acid synthase and cancer: new application of an old pathway. Cancer Res 2006;66:5977–5980.

Liver INTERNATIONAL
OFFICIAL JOURNAL OF THE INTERNATIONAL ASSOCIATION FOR THE STUDY OF THE LIVER

Liver International ISSN 1478-3223

CLINICAL STUDIES

dUTP pyrophosphatase expression correlates with a poor prognosis in hepatocellular carcinoma

Hajime Takatori[1], Taro Yamashita[1], Masao Honda[1], Ryuhei Nishino[1], Kuniaki Arai[1], Tatsuya Yamashita[1], Hiroyuki Takamura[2], Tetsuo Ohta[2], Yoh Zen[3] and Shuichi Kaneko[1]

1 Department of Gastroenterology, Kanazawa University Graduate School of Medical Science, Ishikawa, Japan
2 Department of Gastroenterologic Surgery, Kanazawa University Graduate School of Medical Science, Ishikawa, Japan
3 Pathology Section, Kanazawa University Hospital, Ishikawa, Japan

Keywords
dUTP pyrophosphatase – hepatocellular carcinoma – prognosis – serial analysis of gene expression

Abbreviations
5-FU, 5-fluorouracil; dUTPase, dUTP pyrophosphatase; HCC, hepatocellular carcinoma; IHC, immunohistochemistry; qRT-PCR, quantitative reverse transcription-polymerase chain reaction; SAGE, serial analysis of gene expression.

Correspondence
Masao Honda, MD, Department of Gastroenterology, Kanazawa University Graduate School of Medical Science, 13-1 Takara-Machi, Kanazawa, Ishikawa 920-8641, Japan
Tel: +81 76 265 2233
Fax: +81 76 234 4250
e-mail: mhonda@m-kanazawa.jp

Received 13 August 2009
Accepted 26 October 2009

DOI:10.1111/j.1478-3231.2009.02177.x

Abstract

Background: Hepatocellular carcinoma (HCC) is a malignancy with a poor prognosis, partly owing to the lack of biomarkers that support its classification in line with its malignant nature. To discover a novel molecular marker that is related to the efficacy of treatment for HCC and its biological nature, we performed serial analysis of gene expression (SAGE) in HCC, normal liver and cirrhotic liver tissues. *Methods:* Gene expression profiles of HCC tissues and non-cancerous liver tissues were obtained by SAGE. Suppression of the target gene by RNA interference was used to evaluate its role in HCC *in vitro*. The relation of the identified marker and prognosis was statistically examined in surgically resected HCC patients. *Results:* We identified significant over-expression of *DUT*, which encodes dUTP pyrophosphatase (dUTPase), in HCC tissue, and this was confirmed in about two-thirds of the HCC samples by reverse-transcription polymerase chain reaction ($n = 20$). Suppression of dUTPase expression using short interfering RNAs inhibited cell proliferation and sensitized HuH7 cells to 5-fluorouracil treatment. Nuclear dUTPase expression was observed in 36.6% of surgically resected HCC samples ($n = 82$) evaluated by immunohistochemistry, and its expression was significantly correlated with the histological grades ($P = 0.0099$). Notably, nuclear dUTPase expression correlated with a poor prognosis with statistical significance (HR, 2.47; 95% CI, 1.08–5.66; $P = 0.032$). *Conclusion:* Taken together, these results suggest that nuclear dUTPase may be a good biomarker for predicting prognosis in HCC patients after surgical resection. Development of novel dUTPase inhibitors may facilitate the eradication of HCC.

Hepatocellular carcinoma (HCC) is the fifth most common malignancy and the third leading cause of cancer-related death worldwide (1). Several risk factors are responsible for HCC development, including alcoholism, aflatoxin and genetic diseases such as haemochromatosis and α-1 antitrypsin deficiency; however, the major risk factor is chronic hepatitis owing to hepatitis B virus (HBV) or hepatitis C virus (HCV) infection (2–4). Several treatment options are currently available for HCC management, which include liver transplantation, surgical resection, percutaneous ethanol injection, radiofrequency ablation, transcatheter arterial chemoembolization and systemic or local chemotherapy, and optimal treatment is determined based on tumour stage and liver function (5, 6). However, more than 80% of HCC cases develop advanced HCC after initial treatment (7).

Various chemotherapeutic drugs have been investigated for their antitumour activity in advanced HCC. For example, 5-fluorouracil (5-FU), a thymidylate synthase inhibitor, was the first reported drug studied for the treatment of advanced HCC; however, a median survival rate of 3–5 months has discouraged the further use of 5-FU as a single chemotherapeutic agent (8, 9). Interferon-α (IFN-α) has been reported to have antitumour activity against advanced HCC, and recent reports have suggested the efficacy of a combination of 5-FU/IFN-α for advanced HCC treatment (10–12), although convincing evidence for improved survival rate remains lacking. A recent study has indicated that 16% of advanced HCC patients responded positively to 5-FU/IFN-α treatment with clear and significant survival benefits compared with stable or progressive disease